

Massive expanding torus and fast outflow in planetary nebula NGC 6302

Dinh-V-Trung¹

*Institute of Astronomy and Astrophysics, Academia Sinica
P.O Box 23-141, Taipei 106, Taiwan*

trung@asiaa.sinica.edu.tw

Valentin Bujarrabal

*Observatorio Astronomico Nacional,
Apdo. 112, Alcal de Henares, 28803 Madrid, Spain*

v.bujarrabal@oan.es

Arancha Castro-Carrizo

*Institut de Radioastronomie Millimétrique,
300 rue de la Piscine, 38406 Saint Martin d'Hères, France*

ccarrizo@iram.fr

Jeremy Lim

*Institute of Astronomy and Astrophysics, Academia Sinica
P.O Box 23-141, Taipei 106, Taiwan*

jlim@asiaa.sinica.edu.tw

Sun Kwok

Department of Physics, Hong Kong University, Hong Kong, China

sunkwok@hku.hk

ABSTRACT

¹Center for Quantum Electronics, Institute of Physics and Electronics P.O Box 423, Bo Ho 10000, Hanoi, Vietnam

We present interferometric observations of ^{12}CO and ^{13}CO $J=2-1$ emission from the butterfly-shaped, young planetary nebula NGC 6302. The high angular resolution and high sensitivity achieved in our observations allow us to resolve the nebula into two distinct kinematic components: (1) a massive expanding torus seen almost edge-on and oriented in the North-South direction, roughly perpendicular to the optical nebula axis. The torus exhibits very complex and fragmentated structure; (2) high velocity molecular knots moving at high velocity, higher than 20 km s^{-1} , and located in the optical bipolar lobes. These knots show a linear position-velocity gradient (Hubble-like flow), which is characteristic of fast molecular outflow in young planetary nebulae. From the low but variable $^{12}\text{CO}/^{13}\text{CO}$ $J=2-1$ line intensity ratio we conclude that the ^{12}CO $J=2-1$ emission is optically thick over much of the nebula. Using the optically thinner line ^{13}CO $J=2-1$ we estimate a total molecular gas mass of $\sim 0.1 M_{\odot}$, comparable to the ionized gas mass; the total gas mass of the NGC 6302 nebula, including the massive ionized gas from photon dominated region, is found to be $\sim 0.5 M_{\odot}$. From radiative transfer modelling we infer that the torus is seen at inclination angle of 75° with respect to the plane of the sky and expanding at velocity of 15 km s^{-1} . Comparison with recent observations of molecular gas in NGC 6302 is also discussed.

Subject headings: planetary nebulae: individual (NGC 6302), circumstellar matter

1. Introduction

Low and intermediate-mass stars ($1 M_{\odot} \leq M_{*} \leq 8 M_{\odot}$) evolve through the Asymptotic Giant Branch (AGB) phase, which is characterized by copious mass loss in the form of dusty slow wind, before emerging as planetary nebulae (PNe). The mass-loss process is commonly assumed to be isotropic, resulting in the formation of a spherically symmetric envelope around the central AGB star. However, a significant fraction of the circumstellar envelope around post-AGB stars and planetary nebulae possess bipolar and even multipolar morphology. The mechanisms responsible for such departure from spherical symmetry are still unknown (e.g. Balick & Frank 2002). The interaction between collimated fast outflows and the surrounding envelope or the influence of a binary companion are often cited as possible shaping mechanisms. Large expanding or rotating disks/tori has been frequently inferred to be present in bipolar nebulae such as the Egg Nebula (Sahai et al. 1998) and the Red Rectangle (Bujarrabal et al. 2005). These disks or tori might confine and channel the

wind from the central star into bipolar directions. If the disks/tori are dense enough, the strong interaction (i.e oblique shock) between the wind and the disks/tori could focus and collimate the outflow (Frank et al. 1996). Thus, more detailed studies of the structure and kinematics of such disk/torus could provide better understanding on the formation of the nebulae.

NGC 6302 is a young planetary nebula and belongs to the class of the highest excitation PNe (Pottasch et al. 1996). From the presence of numerous emission lines from highly ionized species, Pottasch et al. (1996) concluded that the central star is a white dwarf or approaching a white dwarf and its excitation temperature is very high, $\sim 380,000$ K. In optical images, NGC 6302 appears as a butterfly shaped nebula with two huge bipolar lobes separated by a dark equatorial lane (Matsuura et al. 2005), which is presumably the location of a massive disk or torus. An expanding HII region is detected at the center of the nebula in the radio continuum (Gómez et al. 1989). The presence of a massive molecular envelope is known through the detection of strong CO rotational lines in NGC 6302 (Huggins et al. 1996, Hasegawa & Kwok 2003). The CO lines have very peculiar and complex shapes, with a double-peaked profile and high velocity wings, extending up to $\sim 40 \text{ km s}^{-1}$ from the systemic velocity. Such line shape suggests that the molecular envelope is likely non-spherical and could contain a fast molecular outflow, similar to fast bipolar outflows observed in some proto-planetary nebulae and young planetary nebulae.

Detailed observations with the VLT and HST of Matsuura et al. (2005) show the presence of a large warped disk oriented perpendicular to the bipolar lobes seen prominently in the optical images. The disk is massive and has a large extinction. Strong emission from crystalline silicates together with PAH bands have also been detected in NGC 6302 (Kemper et al. 2002). We note that, interestingly, OH maser emission, which is usually associated with oxygen rich circumstellar envelopes, has also been detected in NGC 6302 (Payne et al. 1988). Thus, NGC 6302 is chemically peculiar, containing a mixture of carbon-rich and oxygen-rich material.

The distance to NGC 6302 is uncertain, with estimates ranging from 0.15 to 2.4 kpc. From the expansion proper motion of the central HII region, Gómez et al. (1989) estimates a distance of 2.2 ± 1.1 kpc. However, Matsuura et al. (2005) note that a distance much larger than 1 kpc would lead to very high luminosity and shell mass, which would exceed the highest luminosity of post-AGB stars and PNe predicted by stellar evolution models. with even the highest core mass. More recently, Meaburn et al. (2005) detect directly the proper motion of the prominent optical lobes in NGC 6302 nebula and infer a distance of 1 kpc. We will adopt a distance of 1 kpc for NGC 6302, similar to Matsuura et al. (2005) and Kemper et al. (2002).

In this paper we present high angular resolution observations of the $J=2-1$ line of ^{12}CO and its isotope ^{13}CO , in order to study the spatial distribution and kinematics of the molecular gas in the envelope of NGC 6302, especially the massive equatorial disk and the gas moving at higher velocities.

After the submission of our paper for publication, we learned of a recent paper by Peretto et al. (2007), which also presents maps of molecular gas in NGC 6302. Although the spatial distribution of CO emission is similar in both papers, our higher sensitivity (by a factor of 2) observations allow us to produce maps for more velocity channels and better understand the spatial kinematics of the circumstellar envelope. We are able, in particular, to image and study the fast molecular outflows, which are barely detected in lower sensitivity data of Peretto et al. (2007). Where appropriate, we will compare our results with those obtained by Peretto et al. (2007)

2. Observations

We use the Sub-Millimeter Array (SMA), which consists of 8 antennas of 6 m in diameter, to observe NGC 6302. The observation was carried out during the night of May 1, 2006 under excellent weather conditions. The zenith opacity of the atmosphere at 230 GHz was around 0.1, resulting in antenna temperatures (single sideband) in the range of 300 K to 400 K. In our observation the SMA provides projected baselines in the range between 6 m to 78 m. The total on-source integration time of our observation is about 4 hours. The coordinates of NGC 6302 taken from Kerber et al. (2003), $\alpha_{\text{J2000}}=17:13:44.21$, $\delta_{\text{J2000}}=-37:06:15.9$, were used as phase center in our observation. The nearby and relatively strong quasar 1626–298 together with a weaker quasar 1802–396, which is located closer than 1626–298 and to the south of our target source, were monitored frequently to correct for gain variation due to atmospheric fluctuations. Saturn and Jovian moon Ganymede were used as bandpass and flux calibrator, respectively. The large bandwidth (~ 2 GHz) of the SMA correlator allows us to cover simultaneously the ^{12}CO $J=2-1$ line in the upper sideband and the ^{13}CO $J=2-1$ and C^{18}O $J=2-1$ lines in the lower sideband. In our observation the SMA correlator was setup in normal mode, providing a frequency resolution of 0.825 MHz or $\sim 1 \text{ km s}^{-1}$ in velocity resolution. The visibilities are edited and calibrated using the MIR/IDL package, which is developed specifically for SMA data reduction. The calibrated data are then exported for further processing with the MIRIAD package. Continuum emission is subtracted from the visibility data in the uv plane using the task *uvlin* of the MIRIAD package. The resulting line data are then Fourier-transformed to form dirty images. Deconvolution of the dirty images is done using the task *clean*. The resulting synthesized beam for ^{12}CO $J=2-1$ channel maps

is $5''.95 \times 2''.7$ at position angle $\text{PA} = -3^\circ.7$. The corresponding conversion factor between flux and brightness temperature is 1.4 K Jy^{-1} . The rms noise level for each channel of 1 km s^{-1} is 60 mJy beam^{-1} . $^{13}\text{CO } J=2-1$ emission has been also detected and imaged. For the sake of clarity, the channel maps of ^{12}CO and $^{13}\text{CO } J=2-1$ are presented in Figures 1 and 2 with a lower velocity resolution of 2 km s^{-1} . The $\text{C}^{18}\text{O } J=2-1$ line is found to be very faint and the emission could be mapped only around -40 km s^{-1} LSR. Therefore, we will not discuss this line any further in this paper.

We have searched the JCMT archives at the CADC for CO $J=2-1$ observations of NGC 6302. We found usable observations, which were carried out on August 26, 1999. To convert the scale of the archival data in the antenna temperature T_{A}^* , which has been corrected for the atmospheric absorption, to main beam temperature T_{mb} , we used the relation $T_{\text{mb}} = T_{\text{A}}^* / \eta_{\text{mb}}$, assuming a value of 0.69 for the main beam efficiency η_{mb} , similar to Hasegawa & Kwok (2003). After convolving the SMA $^{12}\text{CO } J=2-1$ channel maps to the same angular resolution of 20 arcsec as the JCMT, we find a peak brightness temperature of $\sim 2 \text{ K}$ for the $^{12}\text{CO } J=2-1$ emission. By comparison with the peak main beam temperature of $\sim 2.3 \text{ K}$ for the JCMT spectrum of the same line, we estimate that our SMA observation recovers more than 80% of the $^{12}\text{CO } J=2-1$ flux from NGC 6302.

We also form the continuum image by averaging line free channels in the upper sideband. The rms noise level of the continuum image is $7.5 \text{ mJy beam}^{-1}$. The synthesized beam is $5''.6 \times 2''.3$ at position angle $\text{PA} = -2.5^\circ$.

3. Results

3.1. 1.3mm Continuum emission

We detected and resolved the continuum source at the center of NGC 6302. The map of the continuum emission is shown in the right bottom panel of Figure 1. The continuum emission is extended and elongated in the North-South direction. The position of the continuum peak (flux of $\sim 0.5 \text{ Jy beam}^{-1}$) is $\alpha_{\text{J2000}} = 17:13:44.496$, $\delta_{\text{J2000}} = -37:06:11.936$ and coincides with the location of the free-free emission from ionized gas mapped previously by Gómez et al. (1989) at 6cm. The deconvolved size at half maximum of the continuum emission is estimated to be $7''.0 \times 4''.8$ at a position angle $\text{PA} = -6^\circ$, comparable to the size of HII region mapped by Gómez et al. (1989). The total flux detected by the SMA is about 1.87 Jy. The total continuum flux detected by Hoare et al. (1992) at the similar wavelength of 1.1mm using single dish telescope JCMT is $\sim 1.7 \text{ Jy}$, in good agreement with our measurement. From fitting of the SED in the radio and FIR, Hoare et al. (1992) suggested that

there is no significant contribution from cool dust to the millimeter and centimeter continuum emission, but intensities in that wavelength range are likely to be due to the free-free emission from ionized gas. Therefore, it is very likely that the continuum emission we detect with the SMA originates mainly from the central HII region.

3.2. The molecular torus

In Figure 1 we show the channel maps of the $^{12}\text{CO } J=2-1$ line superposed on the H α image of NGC 6302 (Matsuura et al. 2005). Figure 2 shows the maps of the $^{13}\text{CO } J=2-1$ line. The integrated line profiles of both transitions are given in Figure 3.

The $^{12}\text{CO } J=2-1$ emission clearly shows very complex spatial distribution and several distinct kinematic components. At the systemic velocity, $V_{\text{LSR}} = -33 \text{ km s}^{-1}$, there is a clear central minimum in brightness distribution. The brightest part of the emission appears in channels around the systemic velocity, V_{LSR} from -48 to -20 km s^{-1} , and located spatially close to the 230 GHz continuum emission peak. The CO emitting region is strongly elongated in the North-South direction, similar to the morphology of the continuum emission. The deconvolved size of CO emission at velocity $V_{\text{LSR}} = -38 \text{ km s}^{-1}$ is $10''.8 \times 2''.1$. At velocities from -36 to -32 km s^{-1} , the emission breaks into two separate clumps in the North-South direction, of which the Northern clump dominates in intensity. Toward even more red-shifted velocities ranging from -30 to -18 km s^{-1} the $^{12}\text{CO } J=2-1$ emission still maintains the overall North-South elongated shape but displays noticeable positional shift of the emission centroid toward the center of the nebula at higher redshifted velocities. In the channel maps with velocities in the range -48 km s^{-1} to -33 km s^{-1} , i.e. blue-shifted from the systemic velocity, ^{12}CO emission appears more complex and consists of three extended clumps. Although these clumps are roughly aligned in the North-South direction, the distribution of emission is irregular in comparison to that seen at red-shifted velocities. In the position-velocity diagram along the cut in the North-South direction (see the bottom panel of Figure 4), a clear ring-like structure can be seen between velocities $V_{\text{LSR}} \sim -50$ to -18 km s^{-1} . Our SMA maps of the ^{12}CO emission then indicate that most of the molecular gas essentially occupies an expanding ring perpendicular to the nebula axis. We will then assume that this ring corresponds to an equatorial torus, expanding at low velocity, $\sim 15 \text{ km s}^{-1}$, similar to the circumstellar velocity in AGB stars. This torus would contain most of the molecular gas.

3.3. Fast outflow

In our SMA observations, we also detect ^{12}CO $J=2-1$ emission is at more extreme velocities. At both red-shifted (from about -18 to -10 km s^{-1}) and blue-shifted velocities (from about -75 to -48 km s^{-1}) the emission appears as discrete knots (see Figure 1). The ^{12}CO emission at blueshifted velocities between -75 to -64 km s^{-1} was not detected in previous work of Peretto et al. (2007) due to lower sensitivity (see their Figure 3 and Table 3). We note that the molecular knots detected in our channel maps have more rounded shape, very different from the elongated appearance of the emission from the expanding torus. Such difference is clearly seen in velocity channels at -20 km s^{-1} where the emission mainly comes from the expanding torus, and at -16 km s^{-1} or blue-shifted velocities around -64 km s^{-1} , where discrete knots are located. The properties of these knots can be analysed in more details by examining the position-velocity diagrams. In the position-velocity diagrams of cuts along the East-West direction, all the knots in the blue-shifted high-velocity part of the envelope (denoted as A, B, C respectively in Figure 4) clearly show a linear velocity gradient or Hubble type flow. We note that all these components are located within the optical bipolar lobes of the nebula, but offset from the major nebula axis (East - West direction) and to the South of the central region marked by the continuum emission. Component A, which shows the highest outflow velocity, is very compact and covers a small range in velocity. Such a structure, sometimes termed molecular bullet, has been seen in other young planetary nebulae such as CRL 618 (Ueta et al. 2001) and BD+30°3639 (Bachiller et al. 2000). The Hubble type flow is often seen in young planetary nebulae such as CRL 618 (Sanchez-Contreras et al. 2004). Such flow could result from the interaction between fast collimated outflows from the central star and the ambient gas in the slowly expanding envelope.

3.4. Spatial distribution of ^{13}CO $J=2-1$ emission

Comparison between the channel maps of the ^{13}CO $J=2-1$ emission (Figure 2) and that for the ^{12}CO $J=2-1$ emission (Figure 1) shows that the spatial distribution of ^{12}CO and ^{13}CO is very similar. However, as we will discuss in Sect. 4, the $^{12}\text{CO}/^{13}\text{CO}$ line intensity ratio presents strong spatial variations within the nebula.

4. The molecular gas in NGC 6302

4.1. Temperature

The kinetic temperature (T_k) of the molecular gas detected in our maps can be estimated from the brightness temperature distribution (T_{mb}), particularly for the $J=2-1$ transition. We can see that values as high as $T_{mb} \sim 30$ K are found in the brightest regions. In many channels, we find brightness values larger than 20 K. T_{mb} is approximately equal to $T_k - T_{bg}$ (the cosmic background temperature, 3 K), in the limit of thermalized level populations, high opacities, and resolved spatial distribution. Otherwise, T_k must be larger than $T_{mb} + T_{bg}$, except for very peculiar excitation states. The last condition (resolved spatial structures) is probably not completely fulfilled, since the observed distribution extent is often comparable to the beam size, mainly in the direction of the nebula axis (Sect. 3). Nevertheless, the deconvolved extent of the emitting region is not found to be smaller than the telescope resolution and, except if small-scale clumpiness is present, a high dilution is not expected. As we will show in Sect. 4.2 and 5, the $^{12}\text{CO } J=2-1$ line is likely optically thick and the gas densities are high enough to thermalize the CO low- J lines. Therefore, we conclude that the kinetic temperature in the molecular gas in NGC 6302 is relatively high, typically ~ 30 K or slightly higher.

4.2. CO line opacity

In NGC 6302 the $^{12}\text{CO } J=2-1$ transition is very likely optically thick. This is supported by two observational results: the relatively intense $J=1-0$ line and the relatively high and variable $^{12}\text{CO}/^{13}\text{CO } J=2-1$ intensity ratio.

The $^{12}\text{CO } J=1-0$ transition was observed by Zuckerman & Dyck (1986). Converting to the same beam size as JCMT, the $^{12}\text{CO } J=1-0$ spectrum has a main beam temperature of ~ 1.7 K, which is comparable in strength to the JCMT spectrum (~ 2.3 K) or our JCMT-scale spectrum (see Sect. 2) of the $^{12}\text{CO } J=2-1$ line. As a result, the intensity ratio of $^{12}\text{CO } J=2-1$ and $J=1-0$ is close to 1. When these lines are optically thin and for the high excitation temperatures deduced in the previous subsection, such an intensity ratio should approach 4 (the ratio of the squares of the upper level J -value for each transition), which is the opacity ratio in the high-excitation limit. The measured line ratio of 1 is clearly incompatible with optically thin emission. We conclude that both $^{12}\text{CO } J=1-0$ and $J=2-1$ lines are optically thick.

Although the $^{12}\text{CO}/^{13}\text{CO } J=2-1$ overall brightness distributions are similar, the inten-

sity ratio significantly varies for the different parts of the nebula. This can be readily seen from the total spectra in main-beam brightness units. Values as low as 2 are reached in the most intense features (-40 to -45 km s^{-1} LSR). In weaker features, particularly in the wing at -55 to -60 km s^{-1} , the ratio reaches values as high as 5. Ratios of ~ 3 are found in particular in the relative maxima at -50 km s^{-1} and at -20 to -25 km s^{-1} . Such a trend of the line ratio, depending on the intensity, is expected if the most intense clumps have the highest opacities. These values of the $^{12}\text{CO}/^{13}\text{CO}$ intensity ratio are, on the other hand, too low to represent the abundance ratio, as would be the case if both lines are optically thin. For instance, in NGC 7027, a similar high-excitation PN with a massive molecular component, the $^{12}\text{CO}/^{13}\text{CO}$ line intensity ratios are ~ 30 (Bujarrabal et al. 2001), closer to the $^{12}\text{CO}/^{13}\text{CO}$ abundance ratios often found in evolved-star nebulae.

4.3. Mass of the relevant components

We have calculated the mass of the molecular gas emitting at various velocity ranges, using the method described by Bujarrabal et al. (2001). We have used the $^{13}\text{CO } J=2-1$ line, assuming optically thin emission, a typical temperature of 30 K, and a ^{13}CO relative abundance of $2 \cdot 10^{-5}$ with respect to H_2 . We assume a distance $D = 1$ kpc (Sect. 1). From discussion in Sects. 4.1 and 4.2, we are confident that the method is reliable and will lead to results comparable to those often obtained from CO data in PNe.

We note that the value of the mass deduced from this formulation depends on the assumed rotational temperature. The minimum value is obtained for temperatures of about 15 K; but for our temperature of 30 K the mass value is also low, $\sim 15\%$ over that minimum. Our mass values may then be lower limits if the temperature is higher than deduced above.

As mentioned in Sect. 3, we have tentatively divided the observed lines in four velocity ranges. The line core extends from -48 to -18 km s^{-1} , probably representing an unaccelerated (or slightly accelerated) remnant of the AGB circumstellar envelope, with systemic velocity of ~ -33 km s^{-1} and a moderate expansion velocity of ~ 15 km s^{-1} . The line wings, for velocities outside these limits, would come from regions significantly disturbed and accelerated during the post-AGB evolution of NGC 6302. The mass values calculated for these regions are summarized in Table 1. The total molecular mass from our $^{13}\text{CO } J=2-1$ data is $0.086 M_{\odot}$. From $^{12}\text{CO } J=2-1$ we would deduce a total mass of $0.016 M_{\odot}$, assuming a relative abundance of $3 \cdot 10^{-4}$ and optically thin emission. The discrepancy between the results from ^{13}CO and ^{12}CO is very probably due to high opacity of the $^{12}\text{CO } J=2-1$ line (Sect. 4.2), we will therefore adopt the mass values derived from $^{13}\text{CO } 2-1$.

The total mass derived from our data of $^{12}\text{CO } J=2-1$ is slightly smaller than the value of $0.022 M_{\odot}$ obtained by Huggins et al. (1996) from this line, after correcting for the difference in the assumed distance; the discrepancy is due to the different temperature (~ 77 K) assumed by Huggins et al.

The molecular mass in NGC 6302 derived by us is comparable to that of the ionized gas mass. Gómez et al. (1989) estimate a mass of $0.02 M_{\odot}$, for the region detected in radio continuum (about $10''$ wide). Using the observations of emission lines from several highly ionized species, Pottasch & Beintema (1999) deduced a mass of $0.1 M_{\odot}$, for an inner region extending $\sim 17''$, and a total mass of about $0.5 M_{\odot}$, including the very outer regions in which the estimate is very uncertain. On the other hand, the molecular mass is smaller than the atomic mass in the PDR detected by Castro-Carrizo et al. (2001), $0.27 M_{\odot}$: NGC 6302 is one of the few PNe in which the PDR photodissociated gas is the dominant component. (Results from other authors are always converted to our distance, 1 kpc.) All together, we estimate that the total gas mass in the NGC 6302 nebula is $\sim 0.4\text{--}0.5 M_{\odot}$.

The values derived above for the total gas mass are compatible with the total mass deduced from dust emission at $25 \mu\text{m}$ by Gómez et al. (1989), $4 \cdot 10^{-3} M_{\odot}$, if we assume a reasonable gas/dust mass ratio of ~ 100 . However, the gas mass values are too low compared to the dust mass estimate by Matsuura et al. (2005), $0.03 M_{\odot}$ obtained by fitting the nebula SED using a spherically symmetric model. This discrepancy might be due to the uncertainty in the SED fitting, the adopted dust opacity or the contribution of dust grains with different sizes.

A major discrepancy exists only when our results are compared with those obtained very recently by Peretto et al. (2007). Peretto et al. estimated a total molecular mass of about $1.4 M_{\odot}$, fitting their CO observations by means of the online CO excitation code RADEX (Schöier et al. 2005). This large discrepancy is probably due to the low CO relative abundance assumed in that paper and the geometry-dependent conversion of the column density provided by RADEX into total molecular gas mass.

We will see an independent derivation of the mass of the molecule-rich nebula in Sect. 5, where a value of about $0.1 M_{\odot}$ is obtained from a sophisticated modelling of the main (probably toroidal) component, including and LVG non-LTE treatment of the excitation. Therefore, the total mass values from both methods are very similar, and as we have seen compatible with other mass estimates.

5. Geometry and kinematics of the molecular torus

In order to better understand the structure of the torus and the excitation of the CO molecules, we have constructed a simple model, using a previously developed radiative transfer code (Chiu et al. 2006). Because the torus is very complex, we do not attempt to fit the observations but simply try to capture its overall geometry and spatial kinematics with our model.

The torus is assumed to be axisymmetric and radially expanding at constant velocity of 15 km s^{-1} . The thickness of the torus is also assumed to be constant with radius. In our code the torus is then projected onto a regular three dimensional grid. The physical conditions of the molecular gas, i.e temperature and gas density, at each grid point are calculated from the specified mass loss rate and temperature profile. We take into account 11 rotational levels (up to $J = 10$) of the CO molecule in its vibrational ground state. The populations on the different rotational levels, which are necessary for the calculation of the line opacity and source function at each grid point, are determined by solving the statistical equilibrium equations within the framework of the large velocity gradient formalism. The collision rates between CO and molecular hydrogen are taken from Flower & Launay (1985) and calculated for different temperatures using the prescription of de Jong et al. (1975). CO intensity is calculated for each line of sight by integrating the standard radiative transfer equation. The local line profile, which is needed to integrate the radiative transfer equation, is determined through the turbulence velocity of the molecular gas. We assume a turbulence velocity of 1 km s^{-1} in the torus. The calculated intensity is then used to form a model image of the CO emission from the torus. To compare with our SMA observation, we convolve the model image using a Gaussian beam of the same size as the synthesized beam. A sketch of our model for the torus is shown in Figure 5 and the parameters used in our model are summarized in Table 2.

Using a constant gas temperature of 30 K in the torus and an abundance $[^{13}\text{CO}/\text{H}_2]$ of 2×10^{-5} , we find that we can reproduce the strength of ^{13}CO line observed with SMA using a mass loss rate of $1.5 \times 10^{-4} M_{\odot} \text{ yr}^{-1}$. We present the predicted channel maps of $^{13}\text{CO } J=2-1$ emission in Figure 6 and the total intensity of this line in Figure 7. Because of the high mass loss rate, the gas density in the torus is substantial, about $2 \times 10^4 \text{ cm}^{-3}$ on average. At this high density, the $J=2-1$ transition is thermalized throughout most of the torus.

As presented in Figure 7, the $^{13}\text{CO } J=2-1$ line profile calculated by our model is strongly double-peaked, similar to the observed $^{13}\text{CO } J=2-1$ line shape shown in Figure 3. We also find that the maximum optical depth in the tangential direction is about 0.3, confirming that the $^{13}\text{CO } J=2-1$ line is really optically thin. The total molecular gas mass derived from our model is $\sim 0.087 M_{\odot}$. This model estimate agrees closely with the estimate of molecular

gas mass in the torus presented in Sect. 4.3.

We infer from our model that the torus is seen at an inclination angle of 75° with respect to the plane of the sky, i.e. very close to edge-on. Comparison between the predicted channel maps of ^{13}CO $J=2-1$ emission from the inclined torus (Figure 6) and our SMA data (Figure 2) show that the model reproduces the observed spatial kinematics between -48 km s^{-1} and -18 km s^{-1} . The centroid of the emission clearly exhibits an East – West positional gradient between the receding half of the torus (redshifted velocity from -33 km s^{-1} to -18 km s^{-1}) and the approaching half of the torus (blueshifted velocity between -48 km s^{-1} and -33 km s^{-1}). Because the bipolar lobes are expected to be oriented perpendicular to the expanding torus, we deduce that the Eastern lobe is closer to the observer, while the Western lobe is pointed away from the observer. In the optical image of NGC 6302 nebula (Matsuura et al. 2005), the Eastern lobe is brighter, suggesting that it is closer to the observer, following the common expectation of elevated extinction/obscuration toward the Western lobe due to the presence of the intervening dust in the torus. Indeed, the extinction inferred from measurement of $\text{H}_\alpha/\text{H}_\beta$ ratio by Bohigas (1994) is larger in the Western lobe, implying that the the Western lobe is located in the far side of the nebula. In addition, long slit spectra of H_α emission line by Meaburn et al. (2005) show that the prominent North-West lobe is inclined by $\sim 13^\circ$ with respect to the plane of the sky and away from the observer. As a result, the inclination angle of the torus and the orientation of the bipolar lobes as inferred from modelling the ^{13}CO $J=2-1$ emission are entirely consistent with previous optical observations.

The three-dimensional and very complex structure of the molecular torus in NGC 6302 becomes evident by a comparison between our simple axisymmetric model and the SMA data. In the receding half of the torus, the southern part of the emission is clearly missing between velocities -32 km s^{-1} to -24 km s^{-1} . The approaching part of the torus has very irregular and disturbed morphology, consisting of several clumps (see Figures 1&2). These clumps form a structure resembling the shape of a warped disk. Extinction by dust associated with the dense molecular gas in this approaching part of the torus would then produce the dark warped disk as seen in the optical images of Matsuura et al. (2005). Clearly, the molecular torus exhibits a very complex and fragmental structure. A more sophisticated 3-dimensional model would be needed to disentangle the real structure of the torus.

The complex structure of the torus is also traced by OH maser emission at 1612 MHz. High angular resolution observation of Payne et al. (1988) shows strong maser emission coincident with the optical dark lane. The maser clump has positional gradient in the North-South direction between -54 km s^{-1} and -35 km s^{-1} . Comparison with our SMA data in Figure 1&2 suggests that the OH maser emission spatially coincides with the peak of

CO emission from the torus and the CO emission component at higher blueshifted velocities between -56 km s^{-1} and -52 km s^{-1} . The North-South positional gradient seen in OH maser emission can also be clearly identified in the ^{12}CO and ^{13}CO $J=2-1$ channel maps (see Figures 2&3) and the position-velocity diagram along the north-south direction (see Figure 4).

The optical extinction of the dark lane deduced from the average density (about $2 \cdot 10^4 \text{ cm}^{-3}$) and the size of the torus (about $1.5 \cdot 10^{17} \text{ cm}$) is $\sim 2 \text{ mag}$ (for a standard A_v – column density conversion). This estimate is compatible with the extinction of the equatorial dark lane measured in the visible, which ranges between 3 and 6 mag (Matsuura et al. 2005). This agreement supports our previous conclusion that the properties of molecular gas and dust components of the dark disk are fully compatible, while the contribution of the very extended dust regions to the total IR emission of the source seems poorly understood.

The large inner radius of the torus as shown by our observations and modelling results suggests that the torus is unlikely to play the role of confining and collimating the outflow from the central star to the bipolar direction. The high velocity molecular knots along the optical bipolar lobes identified in our observations are probably the result of some brief but explosive and highly non-isotropic episodes of mass ejection from the central star.

The torus might be formed by the interaction with a binary companion, which acts to focus the slow and dusty AGB wind from the central star toward the orbital plane. Hydrodynamic simulations by Mastrodemos & Morris (1999) show that a wide binary companion could redirect and concentrate the slow wind to form a radially expanding disk-like structure. The complex morphology of the torus as traced by the CO $J=2-1$ emission is probably the result of subsequent interaction with the high velocity outflow.

6. Conclusions

We have imaged at high sensitivity and high angular resolution the envelope around the young planetary nebula NGC 6302 in ^{12}CO $J=2-1$ and ^{13}CO $J=2-1$ lines. Continuum at 1.3mm wavelength is also imaged and seems to come from the inner HII region.

We find that the very complex molecule-rich nebula is well resolved and can be separated into two components: a massive low-velocity torus seen nearly edge-on and high-velocity knots. The image of the dense torus is very accurately coincident with the dark lane that separates the conspicuous two lobes in the optical image of NGC 6302. The fast knots are located within the optical lobes and show a linear velocity gradient, which is characteristic of fast molecular gas in young planetary nebulae.

We find that the $^{12}\text{CO}/^{13}\text{CO}$ $J=2-1$ brightness ratio is low and varies between 2 and 5, decreasing with increasing line intensity. We conclude that the ^{12}CO $J=2-1$ emission is optically thick over much of the nebula, but that ^{13}CO $J=2-1$ is optically thin in most velocities and lines of sight. Using our observations of this line, we estimate masses for the different components, yielding a total molecular gas mass of $\sim 0.1 M_{\odot}$. We discuss the value of the total mass of the NGC 6302 nebula, including the ionized gas, whose mass is comparable to that of the molecular gas, and the massive PDR, which is probably the dominant component. We find a total mass of $\sim 0.5 M_{\odot}$; but we recall that the very uncertain contribution from very outer layers could be significant.

Using a radiative transfer model we infer that the torus is seen at an inclination angle of 75° with respect to the plane of the sky and expanding at a velocity of 15 km s^{-1} . The mass loss rate is found to be very high, $\sim 1.5 \times 10^{-4} M_{\odot} \text{ yr}^{-1}$, resulting in a dense (average gas density $\sim 2 \times 10^4 \text{ cm}^{-3}$) and a massive torus.

We are grateful to SMA staff for carrying out the observations. We thank an anonymous referee for constructive criticisms that helped to improve our paper significantly. V.B. acknowledges support from the *Spanish Ministry of Education & Science*, project numbers AYA2003-7584 and ESP2003-04957. Help from Sebastien Muller is gratefully acknowledged. This research has made use of NASA’s Astrophysics Data System Bibliographic Services and the SIMBAD database, operated at CDS, Strasbourg, France.

REFERENCES

- Bachiller, R., Forveille, T., Huggins, P.J., Cox, P., Maillard, J.P., 2000, A&A 353, L5
- Balick, B., Frank, A., 2002, ARA&A
- Bohigas, J., 1994, A&A 288, 617
- Bujarrabal, V., Castro-Carrizo, A., Alcolea, J., Sánchez-Contreras, C., 2001, A&A 377, 868
- Bujarrabal, V., Castro-Carrizo, A., Alcolea, J., Neri, R., 2005, A&A 441, 1031
- Casassus, S., Roche, P.F., Barlow, M.J., 2000, MNRAS, 314, 657
- Castro-Carrizo, A., Bujarrabal, V., Fong, D., et al., 2001, A&A 367, 647
- Chiu, P.-J., Hoang, C.-T., Dinh-V-Trung, Lim, J., Kwok, S., Hirano, N., & Muthu, C., 2006, ApJ, 645, 605

- De Jong, T., Chu, S.-I., & Dalgarno, A., 1975, *ApJ*, 199, 69
- Feibelman, W., 2001, *ApJ* 550, 785
- Flower, D. R., & Launay, J. M., 1985, *MNRAS*, 214, 271
- Frank, A., Balick, B., Livio, M., 1996, *ApJ* 471, L53
- Gómez, Y., Moran, J.M., Rodríguez, L.F., Garay, G., 1989, *ApJ* 345, 862
- Gómez, Y., Rodríguez, L.F., Moran, J.M., 1993, *ApJ* 416, 620
- Hasegawa, T.I., Kwok, S., 2003, *ApJ* 585, 475
- Hoare, M.G., Roche, P.F., Clegg, R.E.S., 1992, *MNRAS* 258, 257
- Huggins, P.J., Bachiller, R., Cox, P., Forveille, T., 1996, *A&A* 315, 284
- Kemper, F., Molster, F.J., Jäger, C., Waters, L.B.F.M., 2002, *A&A* 394, 679
- Kerber, F., Mignani, R.P., Guglielmetti, F., Wicenec, A., 2003, *A&A* 408, 1029
- Mastrodemos, N., Morris, M., 1999, *ApJ* 523, 357
- Matsuura, M., Zijlstra, A.A., Molster, F.J., Waters, L.B.F.M, Nomura, H., Sahai, R., Hoare, M.G., 2005, *MNRAS* 359, 383
- Meaburn, J., López, J.A., Steffen, W., Graham, M.F., Holloway, A.J., 2005, *AJ* 130, 2303
- Payne, H.E., Phillips, J.A., Terzian, Y., 1988, *ApJ* 326, 368
- Peretto, N., Fuller, A., Zijlstra, A. A., Patel, N.A., 2007, *A&A*, in press
- Pottasch, S.R., Beintema, D., Dominguez-Rodriguez, F.J., Schaeidt, S., Valentijn, E., Vandenbussche, B., 1996, *A&A* 315, L261
- Pottasch, S.R., Beintema, D., 1999, *A&A* 347, 975
- Sahai, R., Hines, D.C., Kastner, J.H., et al., 1998, *ApJ* 492, L163
- Sánchez-Contreras, C., Bujarrabal, V., Castro-Carrizo, A., Alcolea, J., Sargent, A., 2004, *ApJ* 617, 1156
- Schöier, F.L., van der Tak, F.F.S., van Dishoek, E.F., Black, J.H., 2005, *A&A* 432, 369
- Ueta, T., Fong, D., Meixner, M., 2001, *ApJ* 557, L117

Zuckerman, B., Dyck, H.M., 1986, ApJ 311, 345

Table 1. Different molecular components of NGC 6302 and their masses derived from our ^{13}CO data

component	velocity range (LSR)	mass
dense ring: approaching hemisphere	–48 – –33 km s^{-1}	$0.046 M_{\odot}$
dense ring: receding hemisphere	–33 – –18 km s^{-1}	$0.021 M_{\odot}$
high-velocity flow: approaching knots	–75 – –48 km s^{-1}	$0.016 M_{\odot}$
high-velocity flow: receding knots	–18 – –10 km s^{-1}	$0.002 M_{\odot}$

Table 2. Model parameters of the expanding torus

Parameters	
Expansion velocity	15.0 km s^{-1}
V_{LSR}	-33.0 km s^{-1}
Turbulence velocity	1.0 km s^{-1}
\dot{M}	$1.5 \times 10^{-4} M_{\odot} \text{ yr}^{-1}$
T_k	30K
$[^{13}\text{CO}]/[\text{H}_2]$	2×10^{-5}
Inclination angle	75°
Inner radius (R_{\min})	$5 \times 10^{16} \text{ cm}$
Outer radius (R_{\max})	$2 \times 10^{17} \text{ cm}$
Thickness of the torus	$4 \times 10^{16} \text{ cm}$
Mass of the torus	$0.087 M_{\odot}$

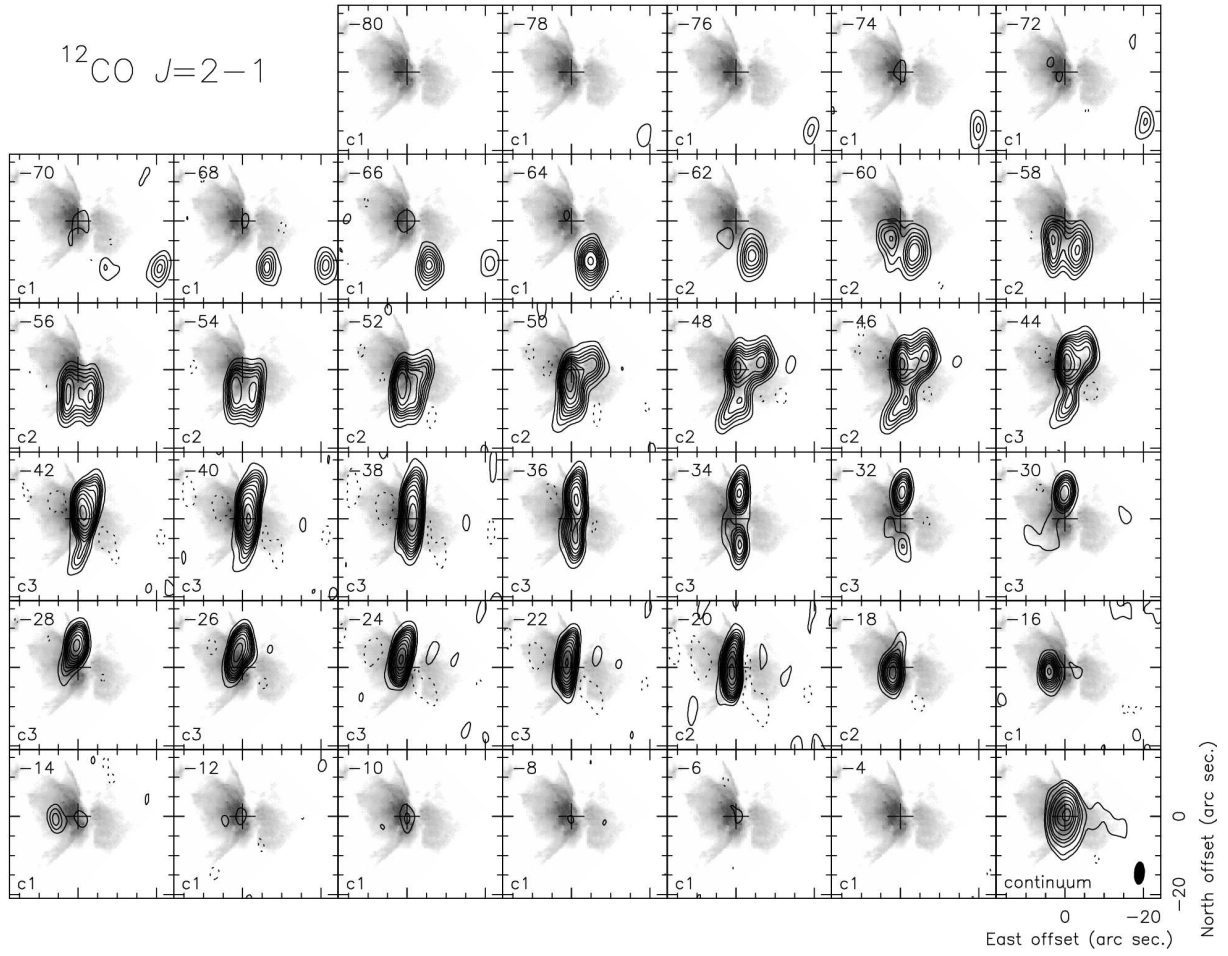


Fig. 1.— Channel maps of $^{12}\text{CO } J=2-1$ emission superposed on the $\text{H}\alpha$ image of NGC 6302 from Matsuura et al. (2005). The LSR velocity is indicated in the upper left of each frame. 230 GHz continuum emission is shown in the lower right frame. The cross on each channel maps denotes the peak position of the 230 GHz continuum emission. The first contours are from 0.2 to 1.6 Jy beam^{-1} by step of 0.2 Jy beam^{-1} for “c1” channels, from 0.4 to 1.6 Jy beam^{-1} by 0.4 Jy beam^{-1} for “c2” channels, and from 0.6 to 1.6 Jy beam^{-1} by 0.6 Jy beam^{-1} for “c3” channels. Other contours are 2.0, 2.4, 3.0, 3.7, 4.8, 6.4, 8.5, 11.5, 15.8 Jy beam^{-1} . Contours for the continuum map are (3, 5, 10, 15, 20, 30, 40, 50, 60) $\times 7.5 \text{ mJy beam}^{-1}$.

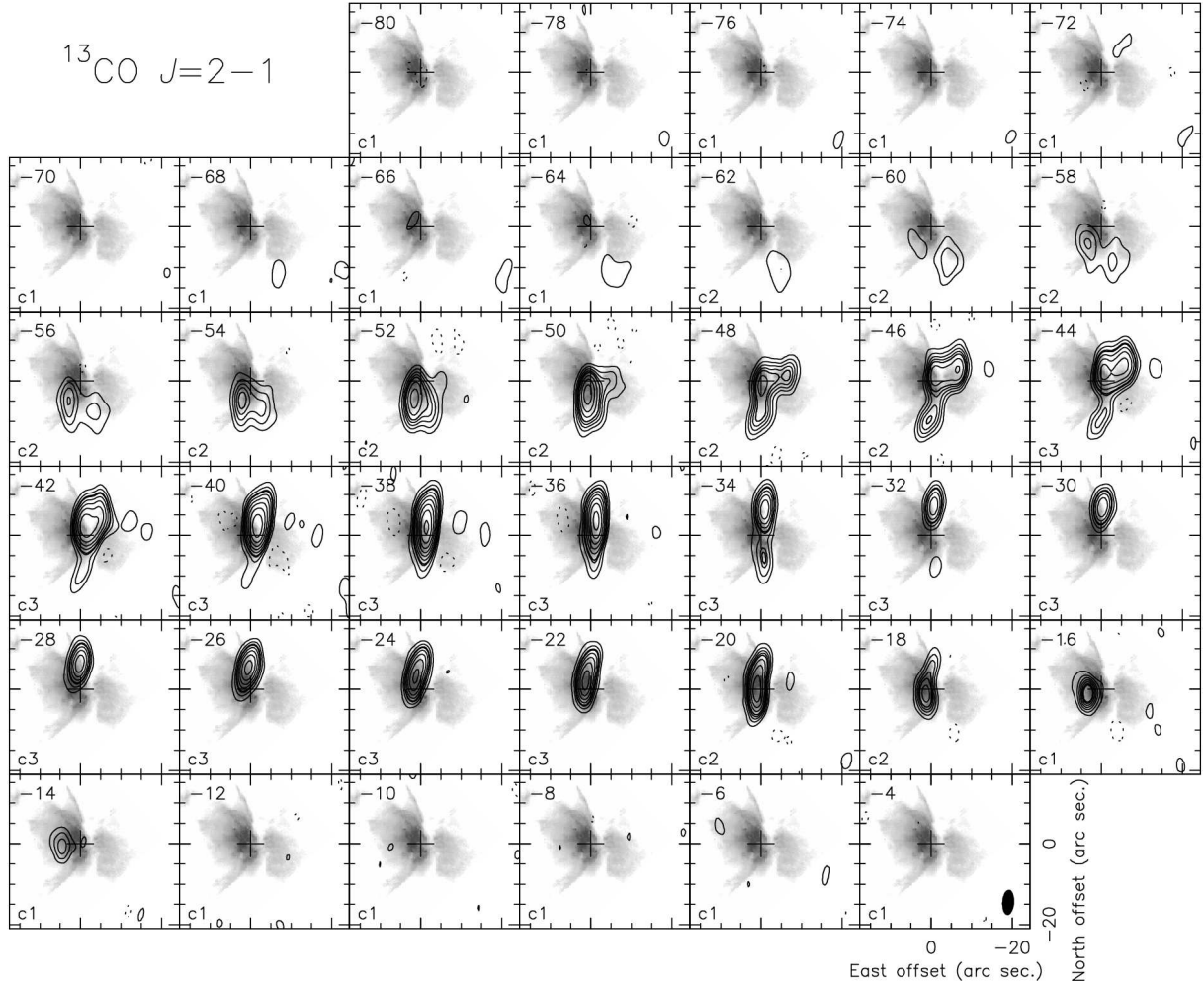


Fig. 2.— Channel maps of $^{13}\text{CO } J=2-1$ emission superposed on the $\text{H}\alpha$ image of NGC 6302. The LSR velocity is indicated in the upper left of each frame. The cross on each channel maps denotes the peak position of the 230 GHz continuum emission. The first contours are from 0.15 to 1.0 Jy beam $^{-1}$ by step of 0.15 Jy beam $^{-1}$ for “c1” channels, from 0.2 to 1.0 Jy beam $^{-1}$ by 0.2 Jy beam $^{-1}$ for “c2” channels and from 0.3 to 1.0 Jy beam $^{-1}$ by 0.3 Jy beam $^{-1}$ for “c3” channels. Other contours are 1.0, 1.4, 2.0, 2.7, 3.8, 5.4, 7.5 Jy beam $^{-1}$.

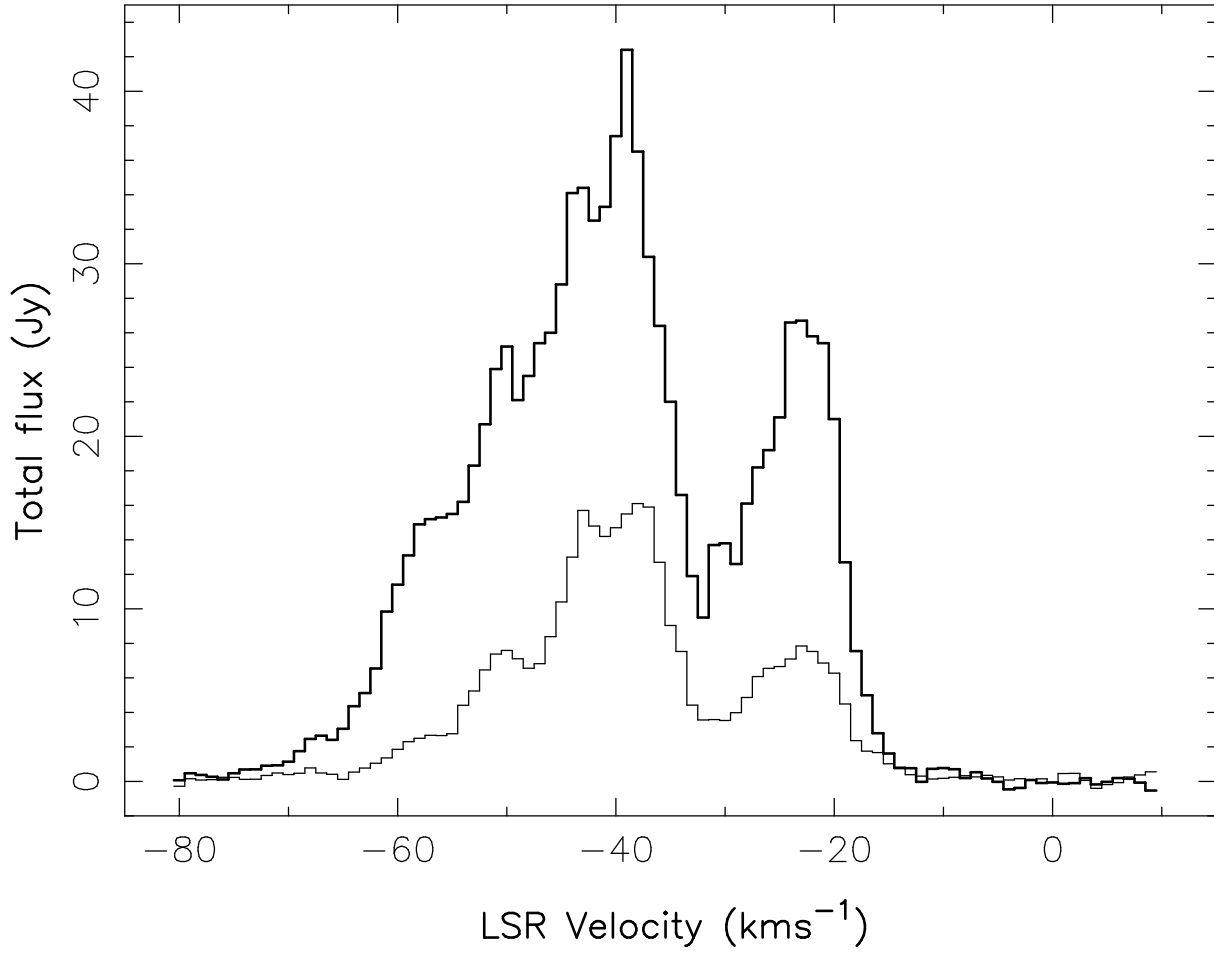


Fig. 3.— Total integrated intensity of ^{12}CO $J=2-1$, shown in thick solid line, and ^{13}CO $J=2-1$ transition, shown in thin solid line, in the SMA observation.

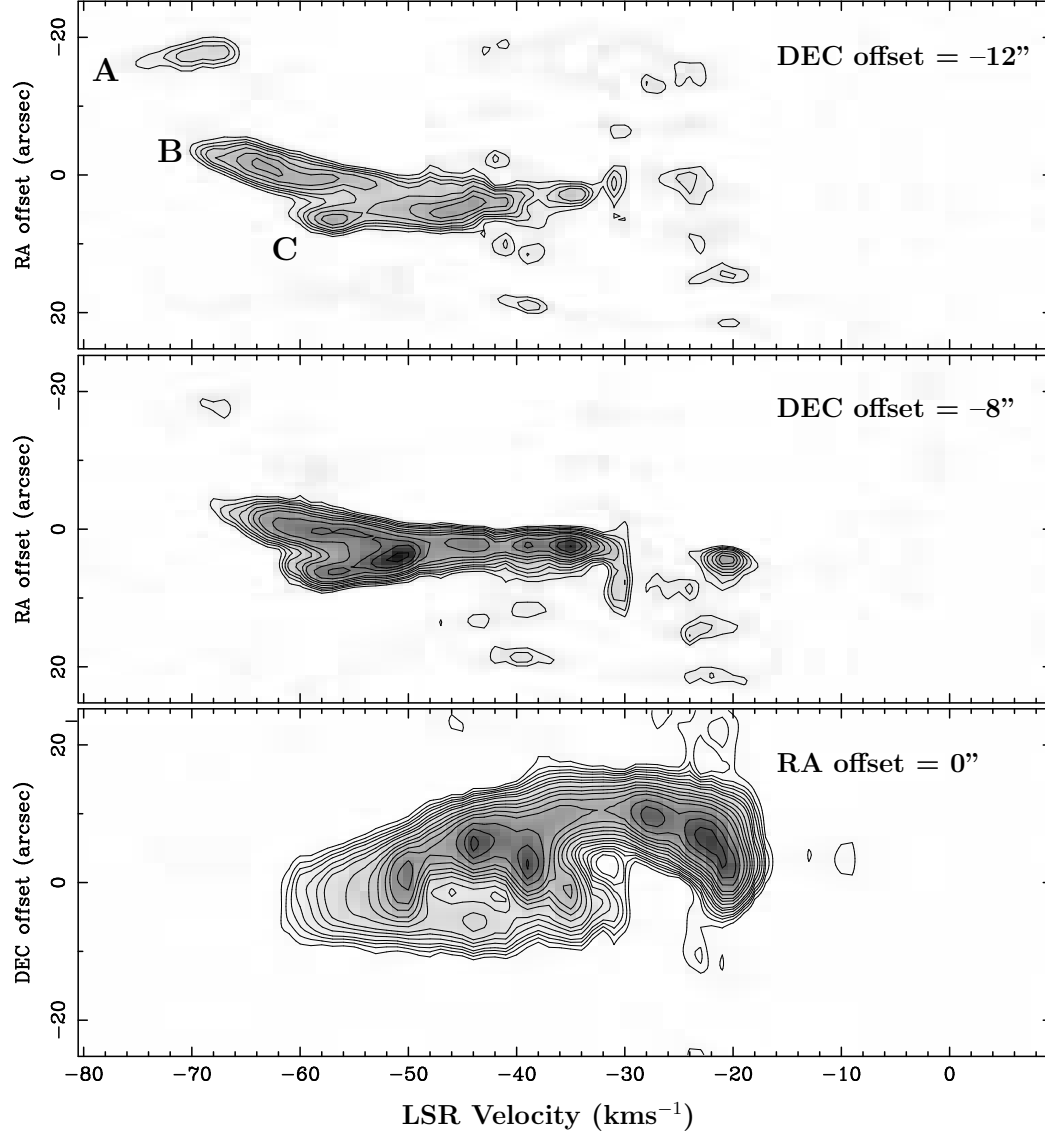


Fig. 4.— Position-velocity maps of $^{12}\text{CO } J=2-1$ along cuts in the East-West direction (upper and middle frames) and in the North-South direction (lower frame). Offset in arcsec from the position of the continuum peak is indicated in the upper-right corner of each frame. The contour levels are $(9, 12, 15, 20, 25, 30, 40, 50, 60, 75, 90, 120, 150, 180) \times 60 \text{ mJy beam}^{-1}$.

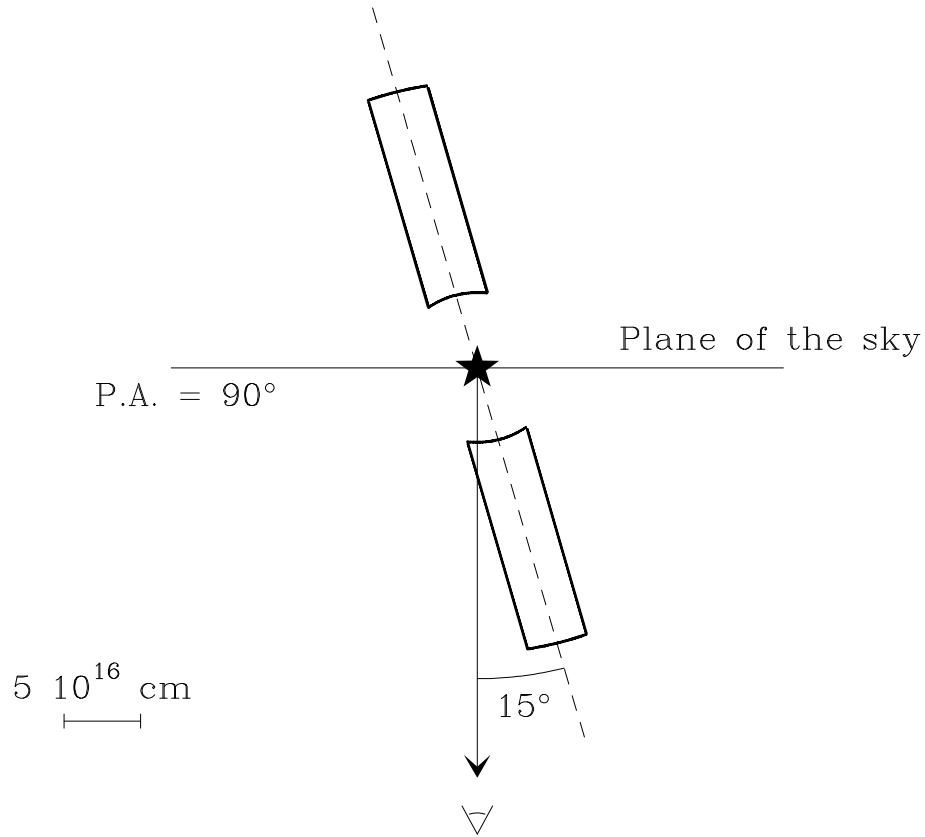


Fig. 5.— Sketch of the model for the expanding torus in NGC 6302.

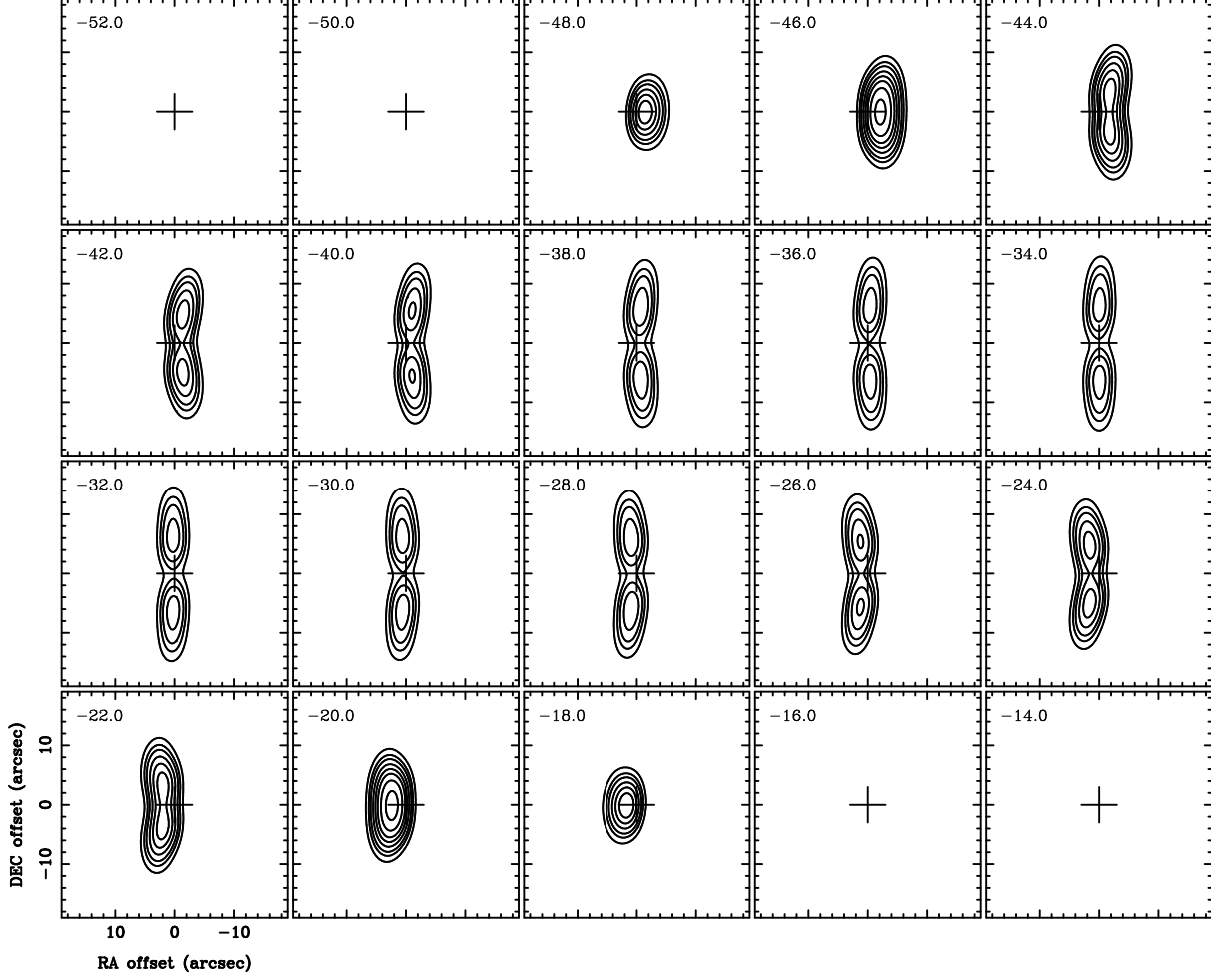


Fig. 6.— Model channel maps of ^{13}CO $J=2-1$ emission from the torus. The LSR velocity is indicated in the upper left of each frame. The cross denotes the center of the nebula, taken to be the peak of the 230 GHz continuum emission. Contour levels are the same as ”c3” in Figure 2, the first contours are from 0.3 to 1.0 Jy beam⁻¹ by 0.3 Jy beam⁻¹ and 1.0, 1.4, 2.0, 2.7, 3.8, 5.4, 7.5 Jy beam⁻¹.

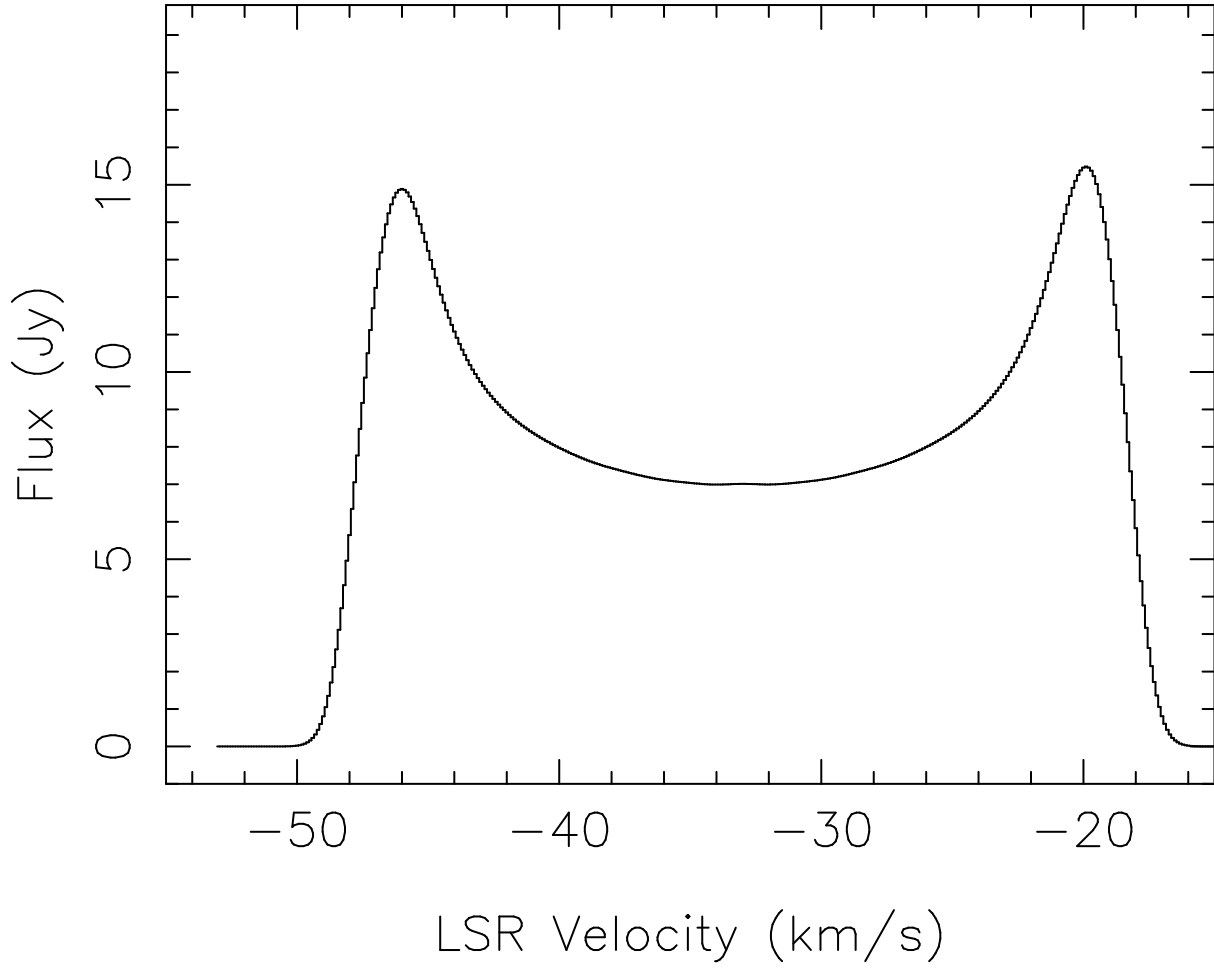


Fig. 7.— Total integrated intensity of ^{13}CO $J=2-1$ emission predicted by our model for the expanding torus.